Title: Group and individual differences in the neural representation of described and experienced risk

Running title: Neural representations of risk

Authors: Loreen Tisdall[1*], Renato Frey[1,2], Andreas Horn[3], Dirk Ostwald[4,2], Lilla Horvath[4], Felix Blankenburg[5], Ralph Hertwig[2], Rui Mata[1,2]

[1]Center for Cognitive and Decision Sciences, University of Basel, Basel, Switzerland.

[2] Center for Adaptive Rationality, Max Planck Institute for Human Development, Berlin, Germany.

[3] Charité – University Medicine Berlin, Movement Disorders and Neuromodulation Section, Berlin, Germany.

[4] Computational Cognitive Neuroscience, Freie Universität Berlin, Berlin, Germany.

[5] Neurocomputation and Neuroimaging, Freie Universität Berlin, Berlin, Germany.

Corresponding author: Loreen Tisdall, Missionsstrasse 60-62, CH-4055 Basel, Switzerland. Email: loreen.tisdall@unibas.ch, phone: +41 61 207 3534

Author contributions: R.M., D.O., A.H. and R.H. designed the research; L.T., L.H., and R.M. acquired the data; L.T. and A.H. analyzed the data; L.T., R.M., R.F., A.H., F.B., and D.O. interpreted the results; L.T., R.F., and R.M. drafted the manuscript; A.H., D.O., L.H., F.B., and R.H. edited the manuscript; L.T., R.F., and R.M. wrote the final version of the manuscript.

Word count (excluding references, tables and figure legends): 5173

Funding: This work was supported by the Swiss National Science Foundation (156172 to R.M., 136227 to R.H.); and the Max Planck Institute for Human Development, Berlin, Germany.

Conflict of Interest: none

Acknowledgements: We thank Laura Wiles for editing the manuscript.

Abstract

Biological markers of risk taking are prominent targets for clinical, developmental, and longitudinal research. With respect to brain function, several regions are considered central for risky choice, yet insights into the neural basis of risk taking stem primarily from studies using single measures. Considering that recent studies suggested different risk-taking measures cannot be used interchangeably, it is currently unclear whether core regions of the brain involved in risk show a measure-dependent functional dissociation. Reporting results from the imaging subsample (N = 116 young adults) of the Basel–Berlin Risk Study, we examine (1) the conjunction of average neural representations of experience-based risky choice in the Balloon Analogue Risk Task and description-based risky choice in monetary gambles, (2) the preservation of individual activation differences across the two measures, and (3) the explanatory power of the neural correlates of risky choice for behavior. Our results suggest common group-level activation increases in nucleus accumbens, inconsistent individual differences in regional activation across measures, and limited explanatory power of neural indices for behavior, within and across measures. Our findings help clarify commonalities and differences between the neural representation of experienced and described risk, and thus should inform research designs targeting individual differences in risk taking.

Keywords: Risk taking, fMRI, BART, gambles, risk matrix

Introduction

Risk preference—whether in the economic sense of preferring high-variance monetary options over more certain ones or, more commonly, preferring options involving uncertain but potentially sizeable negative consequences (Schonberg *et al.*, 2011)—impacts decisions across various life domains, including health, wealth, and criminality (Moffitt *et al.*, 2011; Steinberg, 2013). Past literature offers numerous behavioral measures of risk preference (Appelt *et al.*, 2011; Dohmen *et al.*, 2011), yet recent research suggests these may provide different pictures of individuals' appetite for risk as a function of the different cognitive processes they exploit (Mata *et al.*, 2011; Defoe *et al.*, 2015; Mamerow *et al.*, 2016; van den Bos and Hertwig, 2017; Frey *et al.*, 2017; Pedroni *et al.*, 2017).

One factor contributing to the divergence of behavioral measures resides in how individuals come to know about risk-relevant information: Description- and experience-based measures—henceforth referred to as *described risk* and *experienced risk*, respectively—share central characteristics of decision making under risk (e.g., processing of outcome magnitudes, probabilities and their integration into a subjective value signal informing choice), yet differ with regard to the (coincidental or necessary) involvement of additional cognitive processes, including affect, memory, and learning (Pleskac, 2008; Figner *et al.*, 2009; Hertwig and Erev, 2009; Mata *et al.*, 2011; van Ravenzwaaij *et al.*, 2011). Indeed, experienced risk measures have been proposed to be more ecologically valid because they elicit stronger affective responses as a product of their sequential nature (Schonberg *et al.*, 2011). Perhaps unsurprisingly, described and experienced risk have been found to elicit different choices, leading to different average and individual risk profiles (Mata *et al.*, 2011; Mamerow *et al.*, 2016).

Both described and experienced risk have been used to understand the neural basis of risk preference (Rao *et al.*, 2008; Mohr *et al.*, 2010; Schonberg *et al.*, 2012; Wu *et al.*, 2012; Bartra *et al.*, 2013), yet very few studies have directly compared the two (Pletzer and Ortner,

2016; Blankenstein *et al.*, 2018). Instead, much of our understanding of the neural correlates of risk preference comes from average activation profiles elicited from different measures in between-participant designs. Across such studies, three neural regions have been identified as belonging to a "risk matrix", differentially promoting (*nucleus accumbens* in ventral striatum), inhibiting (*insular cortex*), and controlling (*anterior cingulate cortex*) risky choice (Knutson and Huettel, 2015). However, given the average nature of these results, "risk matrix" regions could present the union of commonly observed risk-related activation patterns, rather than an intersection of all involved regions. But to what extent do different measures of risk preference rely on the same cognitive and neural components? And how are these related to individual differences in risky choice? In the current study, we set out to examine the overlap of neural activation differences in "risk matrix" regions for experienced and described risk.

To understand whether different measures elicit common neural responses, it is crucial to look beyond average (i.e., group-level) activation differences and probe whether activation differences converge between measures at the level of the individual. Owing to the often neglected lack of a match between group-level (i.e., average) and individual-level effects (Blanco *et al.*, 2011; Bornstein *et al.*, 2017), any observed commonality of average neural function in response to described and experienced risk does not necessarily indicate individual-level consistency (Fliessbach *et al.*, 2010). Furthermore, regional activation differences do not necessarily reflect useful, reliable predictors of observed behavior (Poldrack *et al.*, 2018), making it important to evaluate which neural indices of individual differences in described and experienced risk are predictive of choice, within and across measures.

In sum, several neural regions have been proposed as core correlates of risk preference (Knutson and Huettel, 2015), yet it is unclear whether repeated-measures designs of neural activation differences for measures of experienced and described risk result in consistent

neural activation, at group and individual level, and the extent to which neural indices obtained from such measures can account for behavior. This, however, is crucial for our understanding of individual differences in risk preference, especially where neural indices inform studies investigating associated developmental trajectories (Moffitt *et al.*, 2011; Braams *et al.*, 2015) or clinical outcomes (Büchel *et al.*, 2017). To tackle these issues, the current study uses task-dependent neural functional data from the imaging subsample of the Basel–Berlin Risk Study (Frey et al., 2017) in order to examine (1) whether experienced and described risk elicit common group-level activation differences in "risk matrix" regions (i.e., insula, nucleus accumbens, anterior cingulate cortex), (2) whether individual differences for activation in "risk matrix" regions are preserved (i.e., consistent) across the two measures, and (3) the explanatory power of neural indices from "risk matrix" regions for risky choice, within and across measures.

Methods

Participants

We recruited an imaging subsample of 133 young adults from a pool of participants in the Basel–Berlin Risk Study, a large-scale study assessing individual differences, psychometric structure and biological underpinnings of risk preference (for an overview, see Frey *et al.*, 2017 and https://osf.io/rce7g; Dutilh *et al.*, 2017; Pedroni *et al.*, 2017). Exclusion criteria for participation in the magnetic resonance imaging (MRI) session were safety-limiting permanent implants, a history of neurological or psychiatric conditions, usage of psychoactive medication or substances, and receiving psychiatric treatment. After quality control and exclusions (see Supplementary Materials for details), the final sample included in all analyses comprised 116 participants (62 females, mean age at scan = 25.4 years, SD = 2.6 years, range = 20.4–30.1 years).

Ethical approval was obtained from the German Society for Psychology, and the ethics committee of the Center for Adaptive Rationality, Max Planck Institute for Human

Development; this study was conducted in accordance with the stipulated guidelines and regulations.

Experimental measures and procedure

Inside the scanner, participants completed two incentive-compatible risk-taking measures: the Balloon Analogue Risk Task (BART; Lejuez *et al.*, 2002), and monetary gambles (Tom *et al.*, 2007). These were chosen because they are commonly used, relatively simple measures, for which average neural activation profiles (Tom *et al.*, 2007; Rao *et al.*, 2008; Schonberg *et al.*, 2012; Barkley-Levenson *et al.*, 2013) and individual differences have been extensively investigated (Tom *et al.*, 2007; Canessa *et al.*, 2013; Peper *et al.*, 2013; Helfinstein *et al.*, 2014; Braams *et al.*, 2015). Importantly, both measures feature similar concepts including loss, reward, and risk. Yet, whereas these parameters are explicitly described for monetary gambles, some (in particular "risk") must be learned from experience in the BART (Wallsten *et al.*, 2005; Pleskac, 2008). As shown schematically in Figure 1A, the BART involves sequentially inflating a series of virtual balloons in the absence of a priori knowledge about the underlying contingencies. For monetary gambles, individuals make repeated choices between two options: a gamble offering a 50% chance of a gain and a 50% chance of a loss, or a sure outcome of zero (Figure 1B). The individual performance variables of interest were mean number of pumps for the BART, and proportion of accepted gambles for monetary gambles. For further details on the two neuroimaging measures, other measures collected, the experimental procedure, MRI data acquisition and image preprocessing, see Supplementary Materials.

fMRI model specification

At the individual level, we concatenated the two runs for each of the two risk-taking measures, and specified one general linear model (GLM) for the BART and one for monetary gambles. To target the neural representation of risky decisions in both measures, we operationalized risky decisions as the following events: the decision to *Pump* (on reward

balloons) in the BART, and to *Accept* a lottery in monetary gambles. Activation parameter estimates were obtained by convolving event onsets with a canonical hemodynamic response function, filtering out low-frequency components of the time-series data above 128 s (considered to be noise) and correcting for further temporal error autocorrelation by pre-whitening the data using an AR(1) model (Henson, 2003). Movement parameters were entered as covariates.

For our main contrasts of interest—risky versus safe decisions—we operationalized safe decisions as the decision to *Cash out* in the BART, and *Reject* a lottery in monetary gambles. For the BART, we contrasted decisions to *Pump* (on reward balloons) with decisions to *Cash out.* For monetary gambles, we contrasted decisions to *Accept* a lottery with decisions to *Reject*. Given the current focus on neural correlates of decision making under risk rather than correlates of anticipation or feedback-related processes, all analyses involved modeling the time from trial onset (i.e., display of stimulus) until choice (i.e., *Pump/Cash out* for BART or *Accept/Reject* for monetary gambles*)*. At the group level, we specified a flexible factorial design with subject and measure as separate factors in order to obtain statistical parametric maps for mean activation patterns in the two measures and compute a conjunction. See Supplementary Materials for details.

All contrast analyses of neuroimaging data were conducted at the level of the whole brain. Accounting for multiple comparisons, group-level and regression analyses were conducted using a family-wise error (FWE) cluster correction ($p<.05$), with a $p<.001$ uncorrected voxel-wise (peak) threshold. We report the coordinates of local maxima in MNI space (mm). We obtained anatomical labels from the Neuromorphometrics Atlas in SPM8. Results are displayed on a customized study-specific group template, which we created by averaging all normalized structural volumes of all participants.

Overview of statistical analyses

Data and analysis scripts will be made available shortly via the Open Science

Framework; *we will update the document and provide the link here*.

Behavioral data. To examine whether elicited risk taking in the BART and monetary gambles was successful with respect to mirroring behavioral patterns observed in the literature (Tom *et al.*, 2007; Schonberg *et al.*, 2012; Mamerow *et al.*, 2016), we assessed aggregate and individual-level behavior under experienced and described risk via application of two mixed-effects regression analyses to individuals' trial-by-trial performance in the BART and monetary gambles. For the BART, we assessed the effect of balloon capacity and having experienced an explosion on the last trial on risky choice (measured as the number of pumps on experimental balloons in a given trial). For monetary gambles, we assessed the effect of the magnitude of gains and losses on risky choice (measured as binary choice outcome *Accept* or *Reject* in a given trial*)*. Both analyses controlled for the effects of age and gender on risky choice. See Supplementary Materials for details.

Imaging data. We performed confirmatory analyses involving three "risk matrix" regions of interest (ROI) identified by previous work (Knutson and Huettel, 2015); the nucleus accumbens (NAcc), insula, and anterior cingulate cortex (ACC). For each person, we extracted the mean slope for activation differences between risky and safe decisions from the three ROIs, separately for BART and monetary gambles. All ROIs were derived from the Hammersmith atlas (www.brain-development.org). See Supplementary Materials for details. Additionally, we conducted some exploratory whole-brain analyses to ascertain local activation differences for experienced and described risk measures outside the "risk matrix" regions. When reporting the results, we declare exploratory analyses as such.

Group-level conjunction of experienced and described risk. First, we examined group-level neural activations common to both measures as a function of risk (i.e., pumping relative to cashing out in the BART; accepting relative to rejecting an offer for monetary gambles), in particular to see the extent to which joint activation differences occur in NAcc, insula, and ACC. For this purpose, we conducted a whole-brain conjunction analysis of risky

versus safe decisions in the BART and monetary gambles following standard implementation routines in SPM. Specifically, we performed a conjunction analysis over two orthogonal contrasts that tested the conjunction null hypothesis rather than the global null hypothesis, allowing us to infer a conjunction of two effects (risky vs. safe in experienced and described risk) at significant voxels (Friston *et al.*, 2005). We used visualizations of group maps for the BART and monetary gambles to establish whether average brain activity for contrasts of interest were comparable to published functional brain maps and whether our measures could capture typical neural reactions to risk (Tom *et al.*, 2007; Rao *et al.*, 2008; Schonberg *et al.*, 2012; Canessa *et al.*, 2013).

Individual-level consistency of neural activations in "risk matrix" regions for experienced and described risk. Second, we assessed whether individual differences in the neural representation of risky choice were consistent across the two measures. Recall that common activation in response to risk at group level is not necessarily synonymous with consistent individual differences: Even if the majority of individuals shows comparable patterns in each measure, this majority need not be made up of the same individuals. For this purpose, we extracted mean beta values from risky versus safe contrast images obtained for individual-level analyses of the BART (pumps vs. cash out) and monetary gambles (accept vs. reject) using "risk matrix" ROIs, and conducted correlational analyses between the neural indices of the two measures (brain–brain associations).

Explanatory power of neural activations in "risk matrix" regions for risky choice. Third, we examined the explanatory power of experience- and description-based risk-related neural activation for risk-taking behavior, within and across measures. We conducted brain–behavior associations focusing on the "risk matrix" ROIs, modeling whether individual differences in the neural response to risky versus safe decision making (1) in the BART were associated with mean number of pumps, (2) in monetary gambles were associated with proportion of accepted gambles, and (3) in the BART were associated with proportion of

accepted gambles in monetary gambles. Given the temporal order of the two measures, we did not test whether neural signal in monetary gambles accounted for BART behavior. We estimated brain–behavior associations by means of linear regression analyses with standardized variables and controlling for age and gender. This procedure yielded partial correlation coefficients for the association between measure-specific mean beta values extracted from the three ROIs and behavioral indices of risk preference in the BART (mean number of pumps) and in monetary gambles (proportion of accepted gambles). In addition, we ran exploratory whole-brain regression analyses to examine the explanatory power of activation differences outside "risk matrix" regions for behavior. For our analyses examining individual differences, we applied family-wise error correction based on four test families, and report which of the associations reach corrected significance thresholds. See Supplementary Materials for further details.

To note, ROI-based brain–behavior associations have come under scrutiny for being based on non-independent indices (Poldrack and Mumford, 2009; Vul *et al.*, 2009). For example, non-independence arises if (1) an ROI is defined *as a result of* analyses of the same data having identified this region as functionally relevant for a behavioral index, or (2) the events for which the neural index is computed are closely tied to the behavioral index (e.g., neural and behavioral index from the same measure). We argue that the ROI-based brain–behavior associations computed in this study do not fall into either category. Recall that all our ROI analyses are based on *structurally* defined regions that were identified *a priori* as a result of independent research on the neural correlates of risk taking, and that our exploratory whole-brain regression analyses were computed after our focal ROI analyses. Furthermore, mean number of pumps and proportion of accepted gambles are widely used behavioral indices for risk taking, and within-measure brain–behavior associations may yield an upper bound for the explanatory power of localized brain activation. Importantly, regional activation differences may not be equally associated with behavior, hence we were interested in the

relative explanatory power of activity in a set of *a priori* regions, and the extent to which their relative contributions change as a function of the measure used.

Results

Behavioral results

Table 1 contains group-based descriptive statistics for behavior in the two fMRI measures. The two outcome variables of interest - mean number of pumps (across reward balloons) for BART, and proportion of accepted gambles for monetary gambles - were approximately normally distributed (Figures 2A and 2B).

Results from the mixed-effects modeling of the BART (Table 2) were in line with previous results (Schonberg *et al.*, 2012; Mamerow *et al.*, 2016), including main effects of gender (b = -0.16, SE = 0.08, p = 0.04) and previous explosion (b = -0.14, SE = 0.03, p < 0.001). As expected, the mean number of pumps was lower for low-capacity (mean pumps = 4.45, SD = 1.06) than high-capacity (mean pumps = 5.50, SD = 1.52) balloons (cf. Schonberg et al., 2012) but this difference did not translate into a significant main effect of balloon capacity (b = 0.03, SE = 0.06, p = 0.70). For monetary gambles, group-level acceptance rates for individual gambles (Figure 2C) were comparable with previous work (Tom *et al.*, 2007). The results from the mixed-effects logistic regression model for monetary gambles yielded a main effect of age (b = -0.60, SE = 0.09, p < 0.001), gender (b = -0.37, SE = 0.19, p = 0.04), magnitude of gain (b = 0.39, SE = 0.02, p < 0.001) and loss (b = -0.84, SE = 0.03, p < 0.001) on individuals' decisions to reject or accept a risky gamble (Table 3).

Examination of risk preference across the two measures revealed a lack of consistency at the level of the individual because proportion accepted in monetary gambles was not significantly associated with mean number of pumps in the BART (r = -0.11, p = 0.24; Figure 2D). The lack of behavioral consistency was not a result of combining the two runs to compute one behavioral index for each task, as risky choice was consistent over the two runs in monetary gambles (r = 0.86, p < 0.001) and the BART (r = 0.63, p < 0.001).

Neuroimaging results

Let us emphasize that both in the BART and monetary gambles, group-level activation differences for risky versus safe decisions (Table 4, Figure 3A and 3B) were in line with previously reported results (Tom *et al.*, 2007; Barkley-Levenson *et al.*, 2013; Pletzer and Ortner, 2016). For further details, see Supplementary Materials. On this basis, we can now begin to analyze how group-level and individual-level activation converges or fails to converge across the two paradigms for measuring risk preference.

Group-level conjunction of experienced and described risk. One of our main goals was to examine the overlap of neural activation differences in response to experienced and described risk, in particular the extent to which joint activity may be observed in the "risk matrix" regions NAcc, insula, and ACC (Knutson and Huettel, 2015). A conjunction analysis of activation differences in response to risky versus safe options in the BART and monetary gambles revealed a common locally restricted risk signal in a small portion of the ventral striatum, the NAcc (Table 4, Figure 3C). Taking a risk thus seems to elicit an average measure-invariant neural signal in NAcc, but not in insula or ACC. Next, we turn to individual-level analyses to investigate whether individual differences in the neural response to risk are preserved across the two measures, and to examine their explanatory power for risky choice.

Individual-level consistency of neural activations in "risk matrix" regions for experienced and described risk. We examined the consistency of neural signal in the NAcc across measures to assess whether being a conjunction region for experience- and description-based risk activation means that the NAcc is informative for individual differences. Contrary to what might be expected, mean activation in NAcc in the BART was not significantly predictive of NAcc activation in monetary gambles (r = -.07, p =.48; Table 5, Figure 4A). Thus, although at the level of the group the two measures converged on NAcc activity, individual differences were not preserved across measures. In other words, we found group-

but not individual-level consistency for experience- and description-based risk-taking (Bornstein *et al.*, 2017).

We also examined the consistency of the neural signal in the remaining "risk matrix" regions. Mean activation in insula and ACC in the BART was significantly predictive of activation differences in ACC and insula in monetary gambles, respectively; these associations, however, were negative (r = -.45 and r = -.46; $p < .001$) rather than the positive correlations required to suggest consistency (Table 5, Figure 4A). These associations remained significant after application of correction thresholds (FWE) for the number of tests.

Explanatory power of neural activations in "risk matrix" regions for risky choice. We used ROI analyses to examine whether activation differences in response to risky choice in the BART were predictive of mean number of pumps, and whether activation differences in response to risky choice in monetary gambles were predictive of proportion of accepted gambles. For the BART, ROI analyses revealed no significant associations (correlation coefficients r between -.19 and .01) between risk-related activation differences and performance as measured by mean number of pumps (Table 5, Figure 4C). In contrast, for monetary gambles, ROI-analyses supported the involvement of "risk matrix" regions in predicting choice in monetary gambles. Specifically, mean activation in NAcc, insula and ACC extracted from *Accept* versus *Reject* decisions in monetary gambles was significantly negatively associated with the proportion of risky gambles accepted ($-0.3 < r < -0.52$, all $p < 0.001$; Table 5, Figure 4B). The links between neural signal and behavior in monetary gambles remained significant after controlling (FWE) for the number of tests conducted.

We were also interested in brain–behavior associations across measures, that is, whether activation differences in the BART were predictive of risky choice in monetary gambles. Using ROI-specific neural signal, mean activation in ACC in BART was significantly positively associated with the proportion of gambles accepted (r = 0.20, p =

0.01; Table 5; Figure 4D), suggesting that control and monitoring processes in the BART account for some variance in risky choice in monetary gambles.

Exploratory whole-brain regression analyses (whole-brain corrected) did not reveal significant brain–behavior associations for the BART or across measures, but revealed a set of neural regions for which the neural signal in monetary gambles was significantly associated with the proportion of accepted gambles (see Supplementary Table S2).

Discussion

In this study we investigated group- and individual-level neural representations of risk for two prototypical measures—the BART and monetary gambles—to systematically understand which components of the neural response to risk are measure-(in)variant, and investigate the extent to which neural indices explain individual differences within and across measures.

At group level, our conjunction results in NAcc support the notion of a measure-invariant core neural signal of risky choice across experienced and described risk (Knutson and Huettel, 2015). The striatum in general has been implicated in reward processing (Preuschoff *et al.*, 2006; Izuma *et al.*, 2008); to the extent that risk-taking is driven by the motivation to achieve a reward (Ravert *et al.*, 2018), striatal activation is a common neural correlate of risk taking (Tom *et al.*, 2007; Schonberg *et al.*, 2012; Knutson and Huettel, 2015). Note that an alternative explanation for a common NAcc signal for experienced and described risk is the proposed role of the ventral striatum in the coding of prediction error (Hare *et al.*, 2008). Unfortunately, the two measures do not allow us to disentangle these different choice-relevant signals, leaving open the possibility that the main commonality between experience- and description-based risk taking may be comparison of the current option with the status quo.

In turn, the observed group-level activation differences in insula for the BART, but not monetary gambles, support the argument that experienced risk involves potentially more

affective and motivational processes compared with described risk (Hertwig and Erev, 2009; Schonberg *et al.*, 2011). Indeed, the insula is heavily implicated in signaling subjective feelings and explicit motivation (Namkung *et al.*, 2017), and is thought to inhibit risky choice (Knutson and Huettel, 2015). In this study, the feedback involved in the BART, but not monetary gambles, may have involved additional motivational components and led to the observed neural dissociation in insula. One primary contribution of such results is to highlight that although there may be core regions associated with risk preference (Knutson and Huettel, 2015), some may be more "core" than others, depending on the measure used.

Concerning the issue of individual differences, past work has made clear that group averages are not necessarily reflective of individual-level behavioral (Blanco *et al.*, 2011; Bornstein *et al.*, 2017) or neural (Fliessbach *et al.*, 2010) patterns. We examined whether individual differences in neural activation are preserved across two measures and documented a lack of consistency of individual differences in neural activation for risky versus safe decisions under experienced and described risk. Specifically, although, on aggregate, joint activation increases were localized in NAcc across the two measures, individual differences in NAcc activation were not preserved from BART to monetary gambles. Examination of further regions previously identified as core functional correlates of risk and risk preference (Knutson and Huettel, 2015), i.e., insula and ACC, also failed to yield consistent (i.e., positively correlated) individual differences across measures. Although the mechanisms underlying group-level convergence but individual-level divergence (Hedge *et al.*, 2017) can be debated, the current results suggest that individuals respond very differently to different measures, both behaviorally (Frey *et al.*, 2017) and neurally.

A last major aim was to examine the explanatory power of "risk matrix" regions for risky choice. Our results revealed significant brain–behavior associations within-measure for monetary gambles, but not for the BART. As for individual-level neural effects, the measure-dependent explanatory power arises as a likely consequence of the specific processes afforded

by experienced and described risk (Hertwig and Erev, 2009; Mata *et al.*, 2011). In an experience-based, sequential decision-making measure such as the BART, activation differences in a single region are less likely to be highly correlated with choice because choice depends on many interconnected processes (Pleskac, 2008; van Ravenzwaaij *et al.*, 2011; Schonberg *et al.*, 2011). In contrast, the simple nature of description-based monetary gambles lends itself very well to the use of a choice rule, which, at brain level, is evident in choice-relevant neural signal. Concerning the specific brain–behavior associations identified, the observed associations for ACC and insula were in the expected negative direction (Knutson and Huettel, 2015); the more affect-based inhibition and control-related processes are experienced, the lower the number of risky gambles that are accepted. Further, we found that individuals with an on average lower NAcc signal in response to risky choice accepted a higher proportion of gambles. Intuitively, one may expect the opposite; namely, that higher NAcc (i.e., reward) signal is positively associated with risky choice. It is possible that the observed negative association is a corollary of our payoff matrix not being calibrated to individuals, which may result in choice being less discerning for those who place a similar subjective value on all gambles. Future research could easily address this issue by calibrating payoff matrices, for instance via an adaptive willingness-to-pay measure. Across measures, we obtained a link between ACC activation in the BART and proportion of accepted gambles. Given that ACC activation in the BART was not related to performance in the BART, an out-of-measure link for ACC seems surprising and could also be a sequence effect rather than a robust link between experienced and described risk. Thus, for now, we consider this association an informative starting point for further investigation.

There are some limitations to our study. First, we adopted two prototypical risk-taking measures as examples of experienced and described risk, which limits generalization. Past research, however, suggests that other tasks do not fare much better regarding behavioral consistency (Sharma *et al.*, 2014; Pletzer and Ortner, 2016; Frey *et al.*, 2017; Pedroni *et al.*,

2017), suggesting that other measures would probably not show more extensive convergence at group- and individual level. Nevertheless, implementing additional measures based on experienced (Bechara *et al.*, 1994; Figner *et al.*, 2008) and described risk (Holt and Laury, 2002) could address further interesting questions, including whether the convergence of measures is overall higher for experienced or described risk (Frey et al., 2017) and within the respective classes of experienced versus described risk preference measures.

Second, despite our best efforts to create contrasts targeting the neural risk component in the BART and monetary gambles, risk and reward may not be easily distinguishable because the two components coincided in both measures. This is a special limitation for contrast analyses that average activation differences over particular events (e.g., *Pumps* or *Accept* decisions). One way to disentangle risk from reward is to use parametric analyses that map activation to specific functional forms, such as increases in risk or reward. However, standard implementations of the BART, such as the one used here and elsewhere (Lejuez *et al.*, 2002; Schonberg *et al.*, 2012; Helfinstein *et al.*, 2014; Braams *et al.*, 2015), do not allow for the isolation of risk from reward signal even by using parametric analyses, because risk and reward increase linearly over a given trial. Thus, further task manipulations are required that can disentangle risk from reward in the BART, for example, by introducing different (less correlated) payoff and risk (i.e., probability of explosion) functions. However, it deserves to be pointed out that in many real-world domains payoff (reward) and risk (probability) are negatively correlated (Pleskac and Hertwig, 2014).

Third, our design is prey to order effects because we opted for a fixed task order as randomization would have required splitting the sample into two groups based on order, thus reducing power. Note, however, that the overall level of observed risk taking in the BART and monetary gambles was comparable to previous independent investigations (Tom *et al.*, 2007; Schonberg *et al.*, 2012), risky choice within a task was relatively consistent across the two runs, and correlations between risky choice in the BART and monetary gambles did not

change substantially as a function of run number, overall providing little evidence for order effects.

We would like to put forward two recommendations that arise directly from our results. First, a tempting richness of risk preference measures exists, but, as our results show, measures should not be used interchangeably. Increased transparency in selection criteria will not only help researchers make more informed choices between different risk-taking measures for their studies, but will also push the research community towards establishing a taxonomy of measures and their core biological underpinnings. Secondly, we suggest that whenever feasible, researchers include multiple measures in their designs. This would enable direct comparison of measures and, perhaps more importantly, allow analysis of their shared and unique components, for example, through psychometric modeling (Frey *et al.*, 2017; Harden *et al.*, 2017; Poldrack *et al.*, 2018).

To conclude, many longitudinal, clinical and developmental research designs focus on risk preference as a critical predictor or outcome, and often aim to establish links between individual differences in risk preference and neural structure or function (Moffitt *et al.*, 2011; Braams *et al.*, 2015; Holmes *et al.*, 2016; Büchel *et al.*, 2017). Until recently, neuroimaging studies investigated primarily group-level neural representations of risk and paid less attention to individual differences or measurement convergence. To successfully target individual differences in risk taking and understand the biological underpinnings, a switch is required—especially within neuroscience—from group-level to individual-level research (Foulkes and Blakemore, 2018; Rosenberg *et al.*, 2018), and from single- to multi-measure research (Poldrack *et al.*, 2018). If the ultimate aim is to help individuals navigate an uncertain, risk-laden world and make better choices, we first need to navigate and map the mainly uncharted territory of our risk preference measures.

References

Appelt, K.C., Milch, K.F., Handgraaf, M.J.J., et al. (2011). The Decision Making Individual Differences Inventory and guidelines for the study of individual differences in judgment and decision-making research. *Judgment and Decision Making*, **6**, 252–62

Barkley-Levenson, E.E., Van Leijenhorst, L., Galván, A. (2013). Behavioral and neural correlates of loss aversion and risk avoidance in adolescents and adults. *Developmental Cognitive Neuroscience*, **3**, 72–83

Bartra, O., McGuire, J.T., Kable, J.W. (2013). The valuation system: A coordinate-based meta-analysis of BOLD fMRI experiments examining neural correlates of subjective value. *Neuroimage*, **76**, 412–27

Bechara, A., Damasio, A.R., Damasio, H., et al. (1994). Insensitivity to future consequences following damage to human prefrontal cortex. *Cognition*, **50**, 7–15

Blanco, M., Engelmann, D., Normann, H.T. (2011). A within-subject analysis of other-regarding preferences. *Games and Economic Behavior*, **72**, 321–38

Blankenstein, N.E., Schreuders, E., Peper, J.S., et al. (2018). Individual differences in risk-taking tendencies modulate the neural processing of risky and ambiguous decision-making in adolescence. *NeuroImage*, **172**, 663–73

Bornstein, M.H., Putnick, D.L., Esposito, G. (2017). Continuity and Stability in Development. *Child Development Perspectives*, 1–7

van den Bos, W., Hertwig, R. (2017). Adolescents display distinctive tolerance to ambiguity and to uncertainty during risky decision making. *Scientific Reports*, **7**, 1–11

Braams, B.R., van Duijvenvoorde, A.C.K., Peper, J.S., et al. (2015). Longitudinal Changes in Adolescent Risk-Taking: A Comprehensive Study of Neural Responses to Rewards, Pubertal Development, and Risk-Taking Behavior. *Journal of Neuroscience*, **35**, 7226–38

Büchel, C., Peters, J., Banaschewski, T., et al. (2017). Blunted ventral striatal responses to

anticipated rewards foreshadow problematic drug use in novelty-seeking adolescents. *Nature Communications*, **8**, 14140

Canessa, N., Crespi, C., Motterlini, M., et al. (2013). The functional and structural neural basis of individual differences in loss aversion. *The Journal of Neuroscience*, **33**, 14307–17

Defoe, I.N., Dubas, J.S., Figner, B., et al. (2015). A meta-analysis on age differences in risky decision making: Adolescents versus children and adults. *Psychological Bulletin*, **141**, 48–84

Dohmen, T., Falk, A., Huffman, D., et al. (2011). Individual Risk Attitudes: Measurement , Determinants and Behavioral Consequences. *Journal of the European Economic Association*, **9**

Dutilh, G., Vandekerckhove, J., Ly, A., et al. (2017). A test of the diffusion model explanation for the worst performance rule using preregistration and blinding. *Attention, Perception, and Psychophysics*, **79**, 713–25

Figner, B., Mackinlay, R.J., Wilkening, F., et al. (2008). Affective and deliberative processes in risky choice: Age differences in risk taking in the Columbia Card Task. *Journal of Experimental Psychology*

Figner, B., Mackinlay, R.J., Wilkening, F., et al. (2009). Affective and Deliberative Processes in Risky Choice: Age Differences in Risk Taking in the Columbia Card Task. *Journal of Experimental Psychology: Learning, Memory, and Cognition*, **35**, 709–30

Fliessbach, K., Rohe, T., Linder, N.S., et al. (2010). Retest reliability of reward-related BOLD signals. *NeuroImage*, **50**, 1168–76

Foulkes, L., Blakemore, S.J. (2018). Studying individual differences in human adolescent brain development. *Nature Neuroscience*, 1–9

Frey, R., Pedroni, A., Mata, R., et al. (2017). Risk preference shares the psychometric structure of major psychological traits. *Science Advances*, **3**, 1–13

Friston, K.J., Penny, W.D., Glaser, D.E. (2005). Conjunction revisited. *NeuroImage*, **25**, 661–67

Harden, K.P., Mann, F.D., Grotzinger, A.D., et al. (2017). Developmental Differences in Reward Sensitivity and Sensation Seeking in Adolescence: Testing Sex-Specific Associations With Gonadal Hormones and Pubertal Development. *Journal of Personality and Social Psychology*

Hare, T.A., O'Doherty, J., Camerer, C.F., et al. (2008). Dissociating the role of the orbitofrontal cortex and the striatum in the computation of goal values and prediction errors. *The Journal of Neuroscience*, **28**, 5623–30

Hedge, C., Powell, G., Sumner, P. (2017). The reliability paradox: Why robust cognitive tasks do not produce reliable individual differences. *Behavior Research Methods*, 1–21

Helfinstein, S.M., Schonberg, T., Congdon, E., et al. (2014). Predicting risky choices from brain activity patterns. *Proceedings of the National Academy of Sciences of the United States of America*, **111**, 2470–75

Henson, R. (2003). Analysis of fMRI Time-Series: Linear time-invariant models, event-related fMRI and optimal experimental design. In: R. S. J. Frackowiak, K. J. Friston, C. Frith, et al. (eds). *Human Brain Function*. London: Elsevier, p. 793–822.

Hertwig, R., Erev, I. (2009). The description-experience gap in risky choice. *Trends in Cognitive Sciences*, **817**, 1–7

Holmes, A.J., Hollinshead, M.O., Roffman, J.L., et al. (2016). Individual Differences in Cognitive Control Circuit Anatomy Link Sensation Seeking, Impulsivity, and Substance Use. *Journal of Neuroscience*, **36**, 4038–49

Holt, C.A., Laury, S.K. (2002). Risk Aversion and Incentive Effects. *American Economic Review*, **92**, 1644–55

Izuma, K., Saito, D.N., Sadato, N. (2008). Processing of Social and Monetary Rewards in the Human Striatum. *Neuron*, **58**, 284–94

Knutson, B., Huettel, S.A. (2015). The risk matrix. *Current Opinion in Behavioral Sciences*, **5**, 141–46

Lejuez, C.W., Read, J.P., Kahler, C.W., et al. (2002). Evaluation of a behavioral measure of risk taking: the Balloon Analogue Risk Task (BART). *Journal of Experimental Psychology. Applied*, **8**, 75–84

Mamerow, L., Frey, R., Mata, R. (2016). Risk Taking Across the Life Span: A Comparison of Self-Report and Behavioral Measures of Risk Taking. *Psychology and Aging*, **31**

Mata, R., Josef, A.K., Samanez-Larkin, G.R., et al. (2011). Age differences in risky choice: A meta-analysis. *Annals of the New York Academy of Sciences*, **1235**, 18–29

Moffitt, T.E., Arseneault, L., Belsky, D., et al. (2011). A gradient of childhood self-control predicts health, wealth, and public safety. *Proceedings of the National Academy of Sciences*, **108**, 2693–98

Mohr, P.N.C., Biele, G., Heekeren, H.R. (2010). Neural processing of risk. *The Journal of Neuroscience*, **30**, 6613–19

Namkung, H., Kim, S., Sawa, A. (2017). The Insula: An Underestimated Brain Area in Clinical Neuroscience, Psychiatry, and Neurology. *Trends in Neurosciences*, **40**, 200–207

Pedroni, A., Frey, R., Bruhin, A., et al. (2017). The risk elicitation puzzle. *Nature Human Behaviour*, **1**

Peper, J.S., Koolschijn, P.C.M.P., Crone, E.A. (2013). Development of risk taking: Contributions from adolescent testosterone and the orbito-frontal cortex. *Journal of Cognitive Neuroscience*, **25**, 2141–50

Pleskac, T.J. (2008). Decision Making and Learning While Taking Sequential Risks. *Journal of Experimental Psychology: Learning Memory and Cognition*, **34**, 167–85

Pleskac, T.J., Hertwig, R. (2014). Ecologically rational choice and the structure of the environment. *Journal of Experimental Psychology: General*, **143**, 2000–2019

Pletzer, B., Ortner, T.M. (2016). Neuroimaging supports behavioral personality assessment: Overlapping activations during reflective and impulsive risk taking. *Biological Psychology*, **119**, 46–53

Poldrack, R.A., Monahan, J., Imrey, P.B., et al. (2018). Predicting Violent Behavior: What Can Neuroscience Add? *Trends in Cognitive Sciences*, **22**, 111–23

Poldrack, R.A., Mumford, J.A. (2009). Independence in ROI analysis: Where is the voodoo? *Social Cognitive and Affective Neuroscience*, **4**, 208–13

Preuschoff, K., Bossaerts, P., Quartz, S.R. (2006). Neural Differentiation of Expected Reward and Risk in Human Subcortical Structures. *Neuron*, **51**, 381–90

Rao, H., Korczykowski, M., Pluta, J., et al. (2008). Neural correlates of voluntary and involuntary risk taking in the human brain: An fMRI Study of the Balloon Analog Risk Task (BART). *NeuroImage*, **42**, 902–10

van Ravenzwaaij, D., Dutilh, G., Wagenmakers, E.J. (2011). Cognitive model decomposition of the BART: Assessment and application. *Journal of Mathematical Psychology*, **55**, 94–105

Ravert, R.D., Murphy, L.M., Donnellan, M.B. (2018). Valuing Risk: Endorsed Risk Activities and Motives Across Adulthood. *Journal of Adult Development*, **0**, 1–11

Rosenberg, M.D., Casey, B.J., Holmes, A.J. (2018). Prediction complements explanation in understanding the developing brain. *Nature Communications*, **9**, 1–13

Schonberg, T., Fox, C.R., Mumford, J.A., et al. (2012). Decreasing ventromedial prefrontal cortex activity during sequential risk-taking: An FMRI investigation of the balloon analog risk task. *Frontiers in Neuroscience*, **6**, 1–11

Schonberg, T., Fox, C.R., Poldrack, R.A. (2011). Mind the gap: Bridging economic and naturalistic risk-taking with cognitive neuroscience. *Trends in Cognitive Sciences*, **15**, 11–19

Sharma, L., Markon, K.E., Clark, L.A. (2014). Toward a theory of distinct types of

'impulsive' behaviors: A meta-analysis of self-report and behavioral measures. *Psychological Bulletin*, **140**, 374–408

Steinberg, L. (2013). The influence of neuroscience on US Supreme Court decisions about adolescents' criminal culpability. *Nature Reviews Neuroscience*, **14**, 513–18

Tom, S.M., Fox, C.R., Trepel, C., et al. (2007). The neural basis of loss aversion in decision-making under risk. *Science*, **315**, 515–18

Vul, E., Harris, C.R., Winkielman, P., et al. (2009). Puzzlingly high correlations in fMRI studies of emotion, personality, and social cognition. *Perspectives on Psychological Science*, **4**, 274–90

Wallsten, T.S., Pleskac, T.J., Lejuez, C.W. (2005). Modeling Behavior in a Clinically Diagnostic Sequential Risk-Taking Task. *Psychological Review*, **112**, 862–80

Wu, C.C., Sacchet, M.D., Knutson, B. (2012). Toward an affective neuroscience account of financial risk taking. *Frontiers in Neuroscience*, **6**, 1–10

FIGURE LEGEND

Figure 1. fMRI measures. ***A,*** BART. ***upper row,*** Example cash-out trial. ***lower row,*** Example explosion trial. ***B,*** Monetary gambles. ***upper row,*** Example "Reject" trial. ***lower row,*** Example "Accept" trial.

Figure 2. Behavior in the two fMRI measures. ***A,*** Distribution of mean number of pumps in the BART, collapsed across all risky balloons. ***B,*** Distribution of proportion accepted trials in monetary gambles. ***C***, Payoff matrix overlaid with heatmap showing the observed probability of gamble acceptance in monetary gambles. ***D,*** Association between risky choice in the BART and monetary gambles.

Figure 3. Statistical parametric maps of activation differences obtained for risky versus safe decisions under experienced and described risk. ***A,*** BART, Pumps > Cash out (cluster-level FWE $p<.05$, $k>100$). ***B,*** Monetary gambles, Accept > Reject (cluster-level FWE $p<.05$, $k>100$). ***C,*** Conjunction of joint increased activation differences in response to risky versus safe decisions in the BART (Pumps > Cash out) and monetary gambles (Accept > Reject) (cluster-level FWE $p<.05$). Activation differences are displayed on a customized study-group structural template. *Note:* The right (left) side of the image corresponds to the right (left) side of the brain.

Figure 4. Partial correlations (controlling for age and gender) between mean neural signal extracted from ROIs for the BART contrast (Pumps vs. Cash out), mean neural signal extracted from ROIs for monetary gambles contrast (Accept vs. Reject), mean number of pumps in the BART, and proportion accepted trials in monetary gambles. ***A***, Association between regional neural signals across measures (brain–brain). ***B,*** Brain–behavior association BART. ***C,*** Brain–behavior association monetary gambles. ***D,*** Brain–behavior association across measures. *Note:* NAcc = nucleus accumbens; ACC = anterior cingulate cortex. All

variables were z-standardized prior to plotting and analysis. Intercepts and slopes were estimated using robust regression analyses.

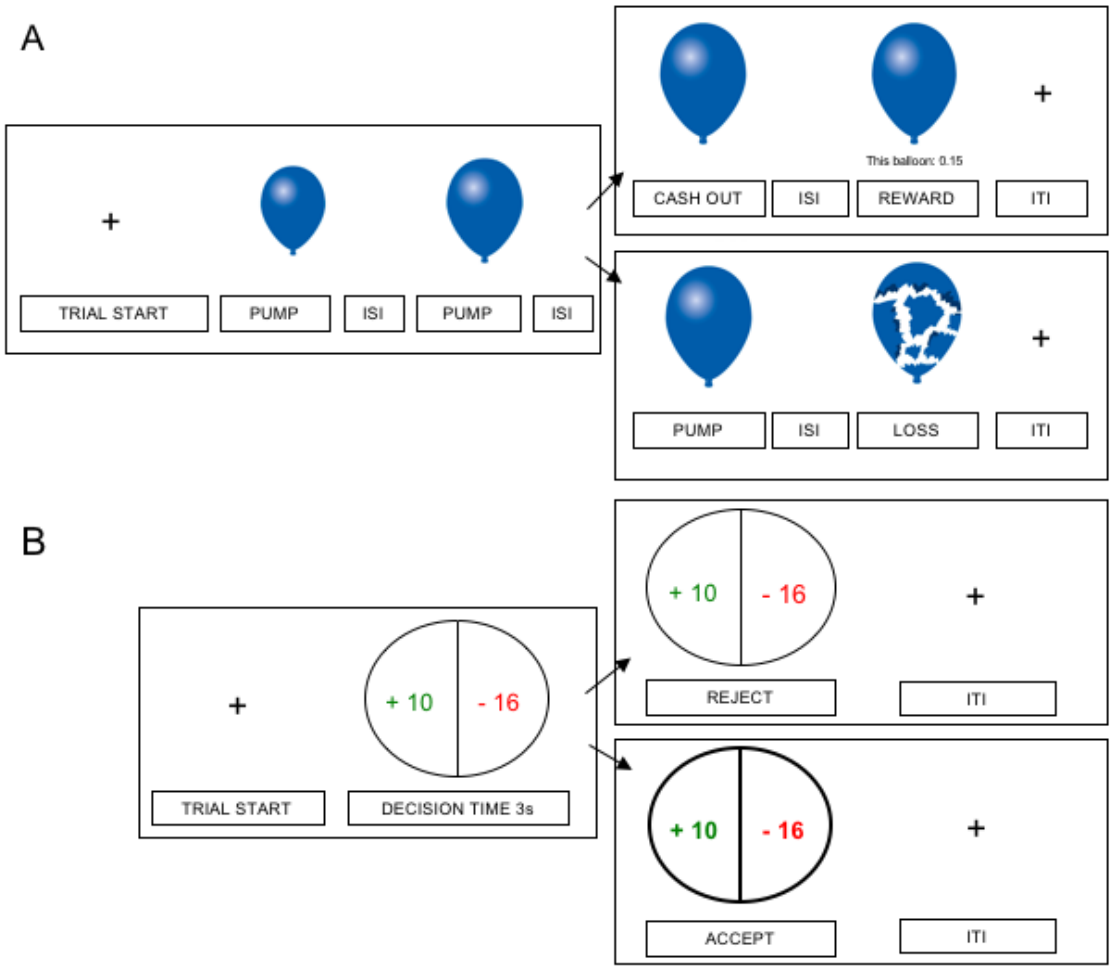

Figure 1. fMRI measures. ***A,*** BART. ***upper row,*** Example cash-out trial. ***lower row,*** Example explosion trial. ***B,*** Monetary gambles. ***upper row,*** Example "Reject" trial. ***lower row,*** Example "Accept" trial.

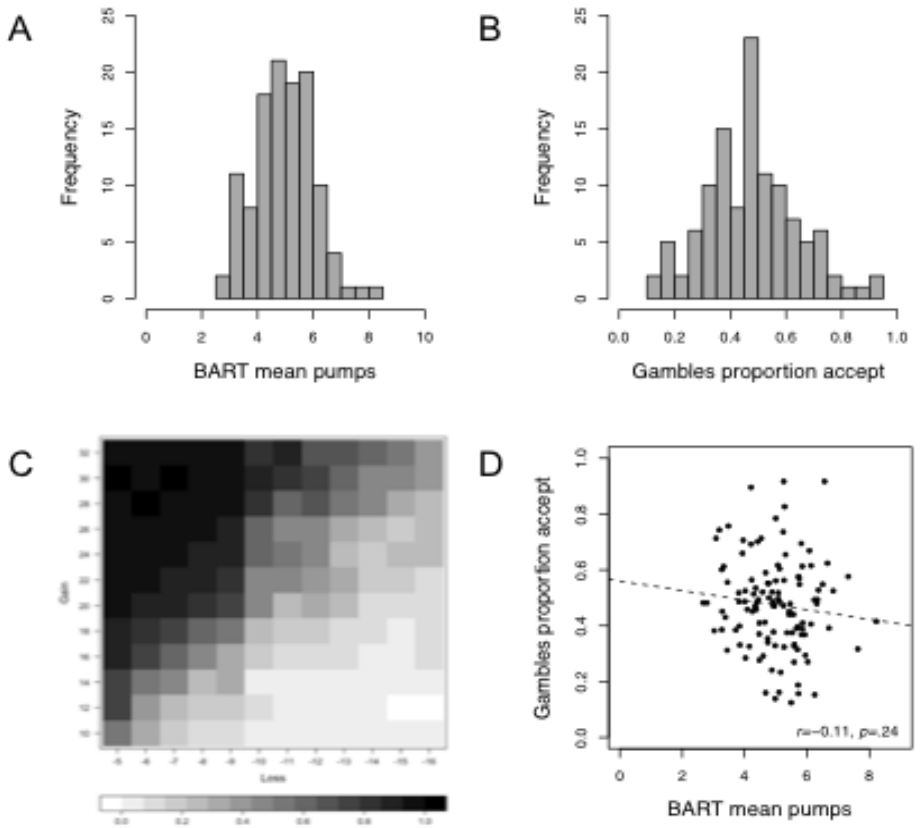

Figure 2. Behavior in the two fMRI measures. ***A,*** Distribution of mean number of pumps in the BART, collapsed across all risky balloons. ***B,*** Distribution of proportion accepted trials in monetary gambles. ***C***, Payoff matrix overlaid with heatmap showing the observed probability of gamble acceptance in monetary gambles. ***D,*** Association between risky choice in the BART and monetary gambles.

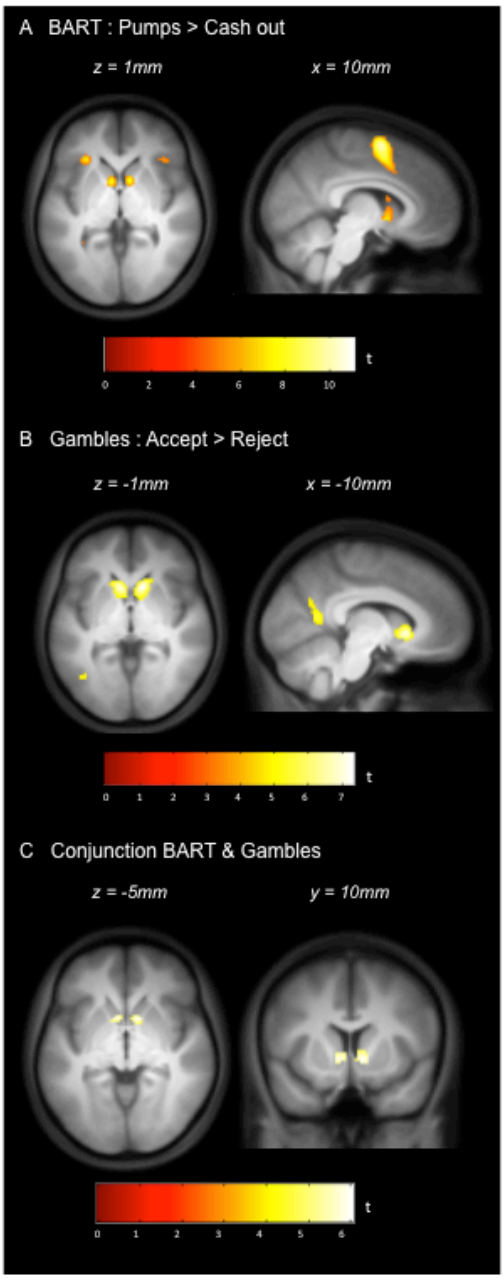

Figure 3. Statistical parametric maps of activation differences obtained for risky versus safe decisions under experienced and described risk. ***A,*** BART, Pumps > Cash out (cluster-level FWE p<.05, k>100). ***B,*** Monetary gambles, Accept > Reject (cluster-level FWE p<.05, k>100). ***C,*** Conjunction of joint increased activation differences in response to risky versus safe decisions in the BART (Pumps > Cash out) and monetary gambles (Accept > Reject) (cluster-level FWE p<.05). Activation differences are displayed on a customized

study-group structural template. *Note:* The right (left) side of the image corresponds to the right (left) side of the brain.

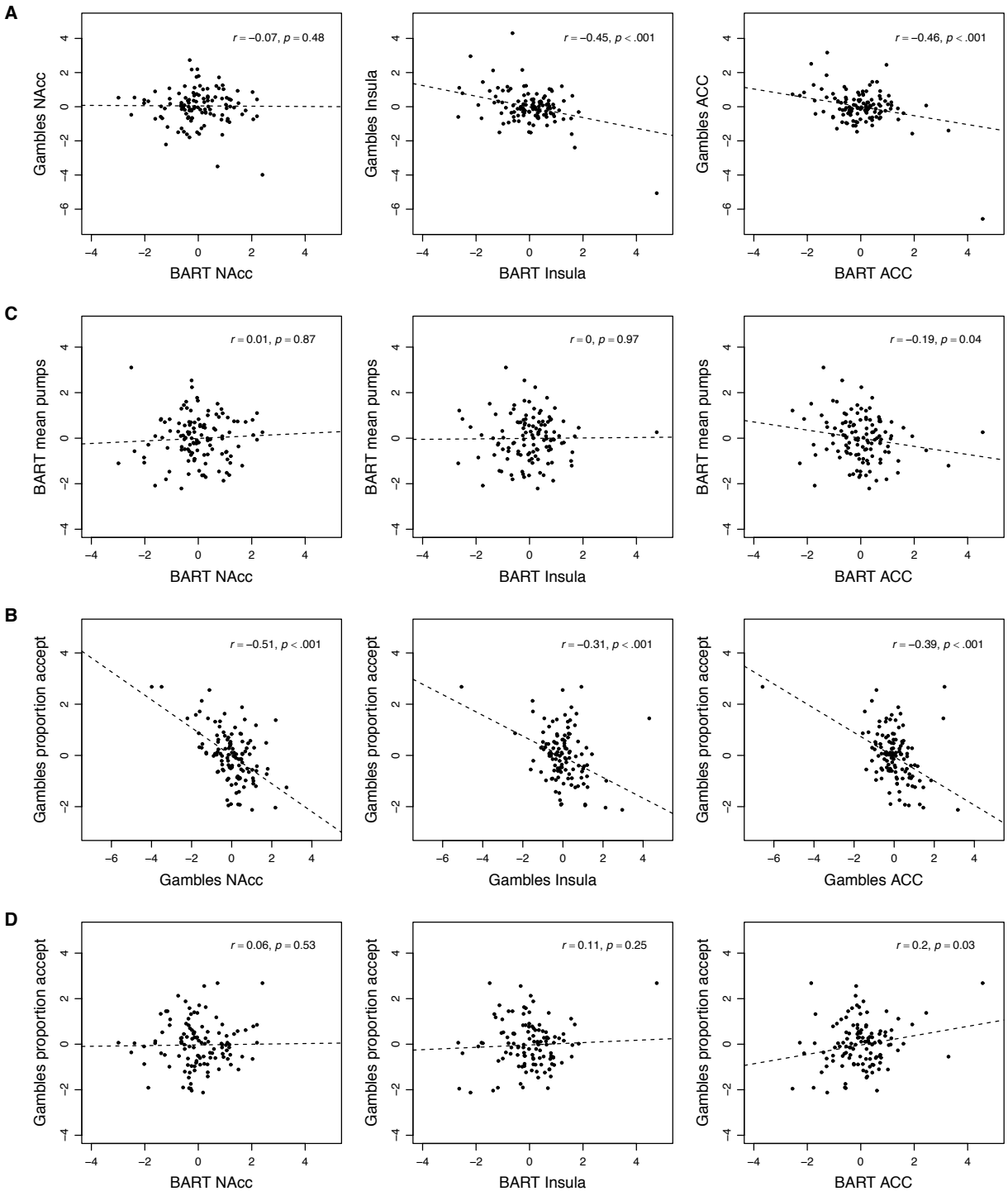

Figure 4. Partial correlations (controlling for age and gender) between mean neural signal extracted from ROIs for the BART contrast (Pumps vs. Cash out), mean neural signal extracted from ROIs for monetary gambles contrast (Accept vs. Reject), mean number of pumps in the BART, and proportion accepted trials in monetary gambles. ***A***, Association between regional neural signals across measures (brain–brain). ***B,*** Brain–behavior association

BART. ***C,*** Brain–behavior association monetary gambles. ***D,*** Brain–behavior association across measures. *Note:* NAcc = nucleus accumbens; ACC = anterior cingulate cortex. All variables were z-standardized prior to plotting and analysis. Intercepts and slopes were estimated using robust regression analyses.

TABLE LEGEND

Table 1. Descriptive statistics for outcome measures for the BART and monetary gambles.

Table 2. Mixed effects linear regression model for trial-by-trial number of pumps in the BART. Age was entered as a continuous variable, sex (0=male, 1=female), capacity (0=12 pumps max, 1=20 pumps max), and explosion on previous trial (0=no, 1=yes) were entered as dichotomous variables.

Table 3. Mixed-effects logistic regression model for trial-by-trial decision making (0 = Reject, 1 = Accept) in monetary gambles. Age, gain, and absolute loss were entered as continuous variables, sex (0=male, 1=female was entered as a dichotomous variable.

Table 4. Significant peak coordinates obtained from group-level contrast analyses for BART and monetary gambles.

Table 5. Partial correlations (controlling for age and gender) between regional (ROI) neural and behavioral indices of risk preference, computed within and across measures.

Table 1. Descriptive statistics for outcome measures for the BART and monetary gambles.

Outcome	Mean (SD)	Range
BART		
Number of completed trials (including controls)	60.72 (6.23)	37–73
Number of low-capacity balloons (max. 12)	20.12 (2.12)	12–25
Number of high-capacity balloons (max. 20)	20.25 (2.20)	12–25
Average pumps on low-capacity balloons (max. 12)	4.45 (1.06)	2.40–6.95
Average pumps on high-capacity balloons (max. 20)	5.50 (1.52)	2.25–9.93
Number of explosions experienced	15.81 (3.81)	6–24
Reaction time pumps control (seconds)	0.62 (0.47)	0.002–15.25
Reaction time pumps risky (seconds)	0.71 (0.53)	0.002–15.09
Reaction time cash out (seconds)	0.90 (0.70)	0.27–11.59
MONETARY GAMBLES		
Number of valid responses	142.67 (1.96)	133–144
Proportion accepted gambles	0.47 (0.16)	0.13–0.92
Reaction time *Accept* decisions (seconds)	1.31 (0.47)	0.46–2.98
Reaction time *Reject* decisions (seconds)	1.30 (0.44)	0.07–2.99

Table 2. Mixed effects linear regression model for trial-by-trial number of pumps in the BART. Age was entered as a continuous variable, sex (0=male, 1=female), capacity (0=12 pumps max, 1=20 pumps max), and explosion on previous trial (0=no, 1=yes) were entered as dichotomous variables.

	Estimate	SE	df	t	p
Intercept	0.16	0.07	136.63	2.44	0.02
Age	0.02	0.04	111.26	0.38	0.70
Sex	-0.16	0.08	111.22	-2.07	0.04
Capacity	0.03	0.06	113.21	0.49	0.63
Explosion on previous trial	-0.14	0.03	111.04	-4.19	< 0.001

Table 3. Mixed-effects logistic regression model for trial-by-trial decision making (0 = Reject, 1 = Accept) in monetary gambles. Age, gain, and absolute loss were entered as continuous variables, sex (0=male, 1=female was entered as a dichotomous variable.

	Estimate	SE	z	p
Intercept	0.52	0.15	3.55	< 0.001
Age	-0.59	0.09	-6.35	< 0.001
Sex	-0.37	0.19	-2.02	0.04
Gain	0.39	0.02	25.73	< 0.001
Loss (absolute)	-0.84	0.03	-25.47	< 0.001

Table 4. Significant peak coordinates obtained from group-level contrast analyses for BART and monetary gambles.

Region	R/L	MNI (mm) x	y	z	T	k
BART: Pumps > Cash out						
Supplementary motor cortex	L	-6	-2	60	11.07	2534
Posterior cingulate gyrus	R	24	-42	14	8.26	206
Nucleus accumbens	L	-6	8	-4	7.84	106
Nucleus accumbens	R	8	8	-4	7.83	137
Anterior insula	L	-30	26	4	7.45	177
Anterior insula	R	40	22	6	7.10	170
Posterior cingulate gyrus	L	-14	-34	20	6.56	131
BART: Cash out > Pumps						
Inferior occipital gyrus	L	-38	-76	-12	20.00	100274
MONETARY GAMBLES: Accept > Reject						
Caudate / Nucleus accumbens	R	10	16	-2	7.31	278
Inferior frontal gyrus (triangular part)	L	-44	34	14	7.00	427
Caudate / Nucleus accumbens	L	-8	16	-2	6.94	209
Angular gyrus	L	-32	-72	36	6.89	1182
Inferior temporal gyrus	L	-50	-66	-12	6.21	449
Supramarginal gyrus	L	-46	-40	40	5.93	358
Precentral gyrus	L	-36	4	26	5.83	165
Middle frontal gyrus	L	-24	14	50	5.58	176
CONJUNCTION Pumps > Cash out & Accept > Reject						
Nucleus accumbens	R	8	12	0	6.03	49
Nucleus accumbens	L	-8	10	-4	5.72	36

All analyses whole-brain, using FWE cluster correction ($p<.05$), with a $p<.001$ uncorrected voxel-wise (peak) threshold; cluster extent threshold $k>100$; controlled for effects of age and gender; k = number of voxels in cluster within which peak coordinate is located. Cluster extent threshold not applied to conjunction analysis.

Table 5. Partial correlations (controlling for age and gender) between regional (ROI) neural and behavioral indices of risk preference, computed within and across measures.

Analysis	Index	NAcc		Insula		ACC	
		b (SE)	***t (p)***	***b (SE)***	***t (p)***	***b (SE)***	***t (p)***
Brain–brain:	Monetary gambles activation ~ BART activation	-0.06	-0.67	**-0.46**	-5.37	**-0.47**	-5.54
		(0.09)	(.50)	(0.09)	**(<.001)**	(0.08)	**(<.001)**
Brain–behavior: Within measures	BART: Mean number of pumps	0.02	0.24	0.04	0.38	-0.17	-1.79
		(0.09)	(.81)	(0.09)	(.70)	(0.09)	(.08)
	Monetary gambles: Proportion Accept	**-0.50**	-5.97	**-0.31**	-3.56	**-0.39**	-4.63
		(0.08)	**(<.001)**	(0.09)	**(<.001)**	(0.08)	**(<.001)**
Brain–behavior: Across measures	Proportion Accept ~ BART activation	0.07	0.75	0.15	1.61	**0.24**	2.61
		(0.09)	(.46)	(0.09)	(.11)	(0.09)	**(.01)**

Note: Estimates obtained from linear regression analyses with standardized outcome and predictor variables. For models within measures, behavioral outcome measures and neural predictors originated from the same measure. For models across measures, the behavioral outcome originated from monetary gambles, and the neural predictors from the BART. ACC = anterior cingulate cortex, NAcc = nucleus accumbens

- SUPPLEMENTARY MATERIALS -

Title: Group and individual differences in the neural representation of described and experienced risk

Authors: Loreen Tisdall, Renato Frey, Andreas Horn, Dirk Ostwald, Lilla Horvath, Felix Blankenburg, Ralph Hertwig, Rui Mata

METHODS

Participants

The participants in this neuroimaging study came from an existing pool of individuals who had participated in the Basel-Berlin Risk Study (BBRS). The BBRS entailed participation in a one-day laboratory session, during which individuals completed an extensive battery of measures assessing individual differences in risk taking (including self-report, frequency, and behavioral measures), cognitive capacity, personality, affect, and genetics (an overview of all subsamples, measures, and further details on the BBRS is reported on https://osf.io/rce7g). The BBRS was run in Basel and in Berlin but for the current study we recruited only individuals from the Berlin site due to the location of the neuroimaging facilities available. The size of the imaging subsample is reflective of oversampling to achieve an effective sample size of N~100 (Yarkoni, 2009) in the event of participant exclusions (e.g., due to excessive head motion in the scanner, image artefacts).

Of the 133 individuals recruited, two participants aborted the session before any functional sequences were collected thus were removed from all subsequent analyses. We excluded a further five participants due to excessive head motion inside the scanner (see image preprocessing section for movement parameter thresholds), one participant due to incidental anatomical findings, four participants due to incomplete data (e.g., only one paradigm was completed inside the scanner), and five participants due to non-compliance with the scanner protocol (e.g., falling asleep, reports of having mixed up button box responses). The final sample included in all analyses comprised 116 participants (62 females, mean age at scan = 25.4 years, SD = 2.6 years, range = 20.4–30.1 years).

Experimental paradigms and additional measures

Inside the scanner, participants completed the Balloon Analogue Risk Task and a monetary gambles task; we describe these measures in more detail below. Outside of the

scanner, we collected self-reported demographic data (date of birth, gender, marital status, educational attainment, native language, and current occupation). Of note, only gender and age at the MRI session (calculated from date of birth) were included as covariates in the current analyses; all other demographic measures were merely collected to describe the sample and ascertain the external validity of our findings with respect to sample characteristics.

As part of an independent project, we assessed individuals' height and weight, collected data from a verbal fluency task, and administered various self-report measures of impulsivity (Schmidt *et al.*, 2008), eating-related behaviors and attitudes (Meermann and Vandereycken, 1987; Pudel and Westenhöfer, 1989; Westenhöfer, 1992); given that these measures were not part of the current analyses, we do not elaborate on these measures here.

Balloon Analogue Risk Task (BART). The BART involves a series of virtual balloons, which individuals are tasked with pumping up in the absence of knowledge about when the balloon will burst. Successful pumps (i.e., pumps that do not lead to a balloon explosion) earn the participant a certain amount of money, but an explosion leads to the loss of the money accumulated on the current trial. Individuals thus make repeated decisions about whether to (1) continue pumping up a balloon (i.e. risky decision), with the prospect of accumulating more money, or (2) stop pumping and cash out any accumulated earnings on a given trial (i.e. safe decision), yet foregoing any further earnings on that trial. Importantly, as individuals move from trial to trial and experience the outcome of their decisions (e.g., a balloon explosion), they can build a mental representation of explosion distributions for a given balloon type over time.

The BART version implemented in the current study featured two risky balloon types and a control balloon. The maximum capacity for the two risky balloons was set to be 12 and 20 pumps, respectively; that is, on average, balloons with a capacity of 12 pumps burst earlier

than balloons with a capacity of 20. Risky balloons were represented in blue and red to discriminate between balloon types based on capacity, with capacity-color assignment being randomized between participants but stable across the two runs. Control balloons were presented in gray, had a maximum capacity of 16, and were added to control for neural processes that required no decision making (e.g., motor or visual). Participants merely inflated control balloons until they disappeared from the screen.

On any given trial, balloon capacity was determined via a random draw from a uniform distribution of values between one and the maximum capacity for the presented balloon type. Participants completed two runs of the BART, with a short break in-between. Each run was programmed to continue for 10 min, after which the final balloon was presented. Given that decisions are made sequentially and may become more difficult as the number of successful pumps in a trial increases, we did not impose a time limit on the decision phase of a given trial, resulting in the number of balloons played varying between individuals (Table 1). Intervals between trials and between successive stimuli within trials were randomized (mean inter-trial interval = 4.39 s, range = 1–11 s; mean inter-stimulus interval = 1.5 s, range = 1–2 s).

The outcome variable typically used in the BART to reflect individuals' risk preference is the average number of pumps administered on cash-out trials only (Lejuez *et al.*, 2002; Wallsten *et al.*, 2005; Rolison *et al.*, 2012; Yu *et al.*, 2016), also referred to as the adjusted average number of pumps. In line with previous research (Mamerow *et al.*, 2016; Frey *et al.*, 2017), in the current study the adjusted average number of pumps was highly correlated with the average number of pumps across all balloons ($r = 0.97$, $p < 0.001$). Given these results, we used the average number of pumps across all balloons as outcome variable in the BART, because it allowed us to retain a maximum number of trials for analysis while working with congruent trial numbers in both neural and behavioral analyses.

It has been suggested that computational models of the BART can help to disentangle different cognitive processes underlying the observed behavior in this task, including gain and loss sensitivity, response consistency, risk preference, or learning (Wallsten *et al.*, 2005; van Ravenzwaaij *et al.*, 2011). However, attempts to model the BART have frequently resulted in highly correlated model parameters and failed parameter recovery (van Ravenzwaaij *et al.*, 2011), suggesting that the purported benefit of using parameters obtained from currently available models may be limited. We set out to model behavior in the BART with two standard models: a target model that assumes a fixed strategy is being used (Pleskac, 2008; Frey *et al.*, 2015) and a Bayesian sequential risk-taking model that allows for dynamic updating processes (Pleskac, 2008). In line with past research the estimation of the model parameters turned out to be unreliable, and we thus do not report the modeling attempt here (a possible reason for the unreliable model parameters may be the lack of strong learning effects). Consequently, we relied on the average number of pumps as a simpler and generic index of risk preference in all subsequent analyses.

Monetary gambles. We further adopted a monetary gambles paradigm with mixed outcomes as an example of a description-based risk-taking measure (i.e., both gains and losses were possible) (Tom *et al.*, 2007; Barkley-Levenson *et al.*, 2013; Canessa *et al.*, 2013; Sokol-Hessner *et al.*, 2013). In the current study, participants made a total of 144 decisions between a sure zero-outcome and a 50/50 gamble. Individual gambles were constructed to populate an asymmetric 12x12 payoff matrix (Figure 1B, right panel) with gains of between 10 and 32 (increments of 2) and losses of between 5 and 16 (increments of 1). Each gamble was presented once, with the order of gamble presentation randomized between participants. On a given trial, once the gamble was presented, participants had 3 s to accept or reject the gamble via respective button presses. Although in previous studies participants gave responses indicating the strength of their decision (Tom *et al.*, 2007; Canessa *et al.*, 2013),

we collected binary responses (accept/reject) only. The rationale for this was that responses under time pressure may bias individuals towards using more extreme responses (Paulhus and Vazire, 2007) and that previously reported analyses were commonly conducted for collapsed (binary) responses (Tom *et al.*, 2007; Canessa *et al.*, 2013). We therefore did not expect a substantial benefit from adopting more fine-grained response options. Participants completed two runs with a short pause in-between, each run featuring 72 gambles. Jitters were introduced between trials (mean inter-trial interval = 4.32 s, range = 1–11 s).

Whereas we computed the proportion of accepted gambles out of all gambles for which a response was provided as an index of risk preference, a simple model that captures sensitivity to gains versus losses has been used to capture decision making for monetary gambles (Tom *et al.*, 2007; Barkley-Levenson *et al.*, 2013; Canessa *et al.*, 2013). However, the critical parameter of this model, loss aversion, was highly correlated with the proportion of accepted gambles (r = -0.9, $p < 0.001$). Consequently, we relied on the proportion of accepted gambles as a simpler and generic index of risk preference in all subsequent analyses.

Experimental procedure

Participants who had previously completed the laboratory session of the BBRS were contacted via phone and informed about the MRI follow-up study. Interested individuals were screened for any contraindications regarding MRI safety. For the current analyses, we did not link participants' data from the laboratory and MRI session, using only data collected during the MRI session. At the time of the MRI session, individuals completed a 2-min training run for the BART and monetary gambles before entering the scanner. The scanner protocol took 75 minutes and included a high-resolution structural scan, two functional sequences for the BART, two functional sequences for monetary gambles, a resting state sequence and a diffusion-weighted imaging sequence. For the current study, only the high-

resolution structural scan and the functional sequences were utilized, with the structural scan only serving normalization purposes during preprocessing of functional imaging data. The resting-state and diffusion-weighted sequences were not part of the current analysis and are not discussed further. The order of scanner sequences was fixed, the BART preceding the gambles task. The risk-taking paradigms were presented using E-Prime 2.0 software (Psychology Software Tools, Pittsburgh, PA), and responses inside the scanner were collected via a COVILEX response box system (series 1.X, Magdeburg, Germany) using the right-hand index and middle finger.

After the MRI session, individuals reported demographic data and completed additional measures reported above. Individuals received a fixed fee of 25 Euro for their participation. In addition, participants could increase their earnings based on performance in the two scanner paradigms. For the BART, participants received 0.05 Euro for each successful pump on a balloon that was cashed out, i.e., did not explode. For monetary gambles, one trial was drawn at random and, if the participant had accepted the trial, was played out. The resulting loss or gain was combined with money made in the BART. Trials which were drawn but which the participant had rejected resulted in a 0 Euro outcome. Participants were told about the incentive structure at the start of the MRI session and received cash earnings at the end of the session (average actual payment = 41.50 Euro, SD = 14.50 Euro).

MRI data acquisition and image preprocessing

Neuroimaging data were collected at the Magnetic Resonance Imaging Laboratory at the Max Planck Institute for Human Development (Berlin, Germany) on a 3T Siemens MRI system with 12-channel head coil. Participants received a magnetization-prepared rapid gradient echo (MP-RAGE) sequence (repetition time = 2500 ms, echo time = 4.77 ms, inversion time = 1100 ms, flip angle = 7 degrees, field of view = 256 × 256 mm^2, 192 slices,

voxel size = 1 × 1 × 1 mm^3). In each of the four functional runs, up to 320 functional T2*-weighted BOLD echo-planar images were acquired for every person (repetition time = 2010 ms, echo time = 30 ms, flip angle = 78 degrees, field of view = 192 × 192 mm^2, voxel size = 3 × 3 × 3 mm^3, 33 transversal slices/volume with 15% distance factor). Image preprocessing and analyses were carried out using standard procedures implemented in SPM8 (http://www.fil.ion.ucl.ac.uk/spm/software/spm8/). Preprocessing involved realignment and co-registration of functional to structural volumes. Volumes were nonlinearly warped into standard stereotactic (MNI) space based on structural scans using the New Segment method (Ashburner and Friston, 2005). To control for spatial noise and average effects that may arise as a function of residual anatomical differences between subjects, images were spatially smoothed using an 8-mm full-width half-maximum Gaussian kernel.

fMRI model specification

BART. To model the neural activation in response to experienced risk in the BART, we specified a first level design matrix for each individual which included the following regressors per run (see Supplementary Figure S1 for an exemplary design matrix): Onset vector of pumps for control balloons, two onset vectors for pumps on reward balloons, onset vector for cash outs, onset vector for explosions, and six motion parameters estimated during the realignment process. We included two onset vectors for pumps on reward balloons to facilitate different analyses. Our main analysis focused on contrasting risky decisions with safe decisions on the BART, which we operationalized as contrasting pumping on risky balloons with the decision to cash out. One potential confound of such a contrast is that there may be systematic biases in the history of trials leading to a cash out decision. Concretely, cash-out decisions may not be similarly distributed across trials with regards to their onset, but perhaps happen early on in the trial as a result of mounting tension or the motivation to ensure some saved earnings. In building a contrast between cash-out events and pump events,

any such systematic biases may also bias the neural signals. To address this issue, for every individual included in the analysis, we isolated the maximum serial position of all cash-out decisions and used this to cap the serial position of pumps included in the first onset vector; we refer to this vector as 'matched pumps'. Onsets for the remaining pumps (i.e., those exceeding the maximum serial position of all cash-out decisions) were included in the second pumps vector; together, the two vectors facilitated supplementary analyses contrasting pumps on all risky (i.e. reward) balloons with pumps on control (i.e., non-reward balloons).

The onset vector for explosions was included in order to account for additional variance, better isolate the main effects of interest, and also remove neural responses to explosions from baseline activity. We did not differentiate between onsets for high- and low-capacity balloons because preliminary analyses in which we contrasted pumps on high-capacity with pumps on low-capacity balloons yielded no significantly different neural activations as a function of balloon type; consequently, we collapsed pumps across high- and low-capacity balloons for all analyses. For this main contrast of interest—risky versus safe decisions—we contrasted cash-out decisions with matched pumps, using the contrast weights [0 1 0 -1 0 0 0 0 0 0 0] to assess *Pumps (matched)* > *Cash out*, and [0 -1 0 1 0 0 0 0 0 0 0] for *Pumps (matched)* < *Cash out*.

Neuroimaging analyses of BART data usually involve contrasting activation differences in response to pumps on reward balloons with pumps on control balloons (Rao *et al.*, 2008; Schonberg *et al.*, 2012; Yu *et al.*, 2016). This procedure, however, does not address the question of risk preference directly because it merely contrasts activation for conditions with and without a decision component thus providing a general picture of the neural correlates of decision making but not risk preference. The ubiquity of contrasting reward and control pumps in the BART in the literature, however, allows for a direct comparison of group-based results originating from different studies. Thus, we supplemented our focal

analysis with a contrast of all pumps on reward versus control balloons. For this supplementary contrast of pumps on reward versus control balloons, we used the contrast weights [-2 1 1 0 0 0 0 0 0 0 0] to compute *Control pumps* < *Reward pumps*, and [2 -1 -1 0 0 0 0 0 0 0 0] to compute *Control pumps* > *Reward pumps*.

Monetary gambles. For the individual-level modeling of monetary gambles decisions, we specified one GLM, which targeted the neural representation of risky versus safe decisions (Barkley-Levenson *et al.*, 2013) and included the following regressors (see Supplementary Figure S2 for an exemplary design matrix): Onset vector for all *Accept* decisions, onset vector for all *Reject* decisions, six motion parameters estimated during the realignment procedure. The simplicity of the paradigm allowed for this comparatively straightforward design matrix with only two regressors of interest, nevertheless yielding clean (event-unrelated) baseline activity. Emulating previous analyses (Barkley-Levenson *et al.*, 2013) and striving for a contrast analysis that is comparable for risk in both the BART and monetary gambles, individuals' *Accept* decisions were contrasted with *Reject* decisions.

To estimate activation differences for risky versus safe decisions in monetary gambles, we used the contrast weights [1 -1 0 0 0 0 0 0] to estimate *Accept* > *Reject*, and [-1 1 0 0 0 0 0 0] to estimate *Accept* < *Reject*.

At the group level, we specified a flexible factorial design with subject and measure as separate factors in order to obtain statistical parametric maps for mean activation patterns in the two measures and compute a conjunction. Within-subject contrast images from risky versus safe decisions in monetary gambles and the BART were entered as two blocks, one block per measure (see Supplementary Figure S3 for design matrix). We assumed independence for the subject and measure factors but equal variance only for the subject factor. Gender and age were entered as covariates of no interest. See Supplementary Materials for details about the design matrices, onset vectors, contrast weights and additional

contrast analyses.

Overview of statistical analyses

Behavioral data. The specification of regression models and selection of predictor variables for both tasks followed previously reported trial-level effects (Wallsten *et al.*, 2005; Tom *et al.*, 2007; Mamerow *et al.*, 2016). To model trial-specific effects on risky choice in the BART, we regressed the number of pumps on experimental balloons (in a given trial) onto average effects of balloon capacity as a proxy for the level of risk (12/20), whether the previous trial ended in an explosion (yes/no), age and sex (0=male, 1=female), allowing for random effects for balloon capacity and previous explosion (nested within individual). For monetary gambles, we specified a logistic mixed-effects model, in which the decision to accept or reject a particular lottery in a given trial was regressed onto average effects of magnitude of the gain, magnitude of the loss, age and sex (0=male, 1=female), as well as individual effects for gain and loss magnitude. Before fitting the models, all continuous variables were normalized and categorical variables dummy-coded. In the BART, number of pumps was normalized separately for each of the two experimental balloon types.

All behavioral analyses were run in R (R Project for Statistical Computing; RRID:SCR_001905 http://r-project.org), using the packages lme4 (lme4: Linear mixed-effects models using Eigen and S4; R package v 1.1–8; http://CRAN.R-project.org/package=lme4) and lmerTest (lmerTest: Tests in linear mixed effects models; R package v 2.0–25; http://CRAN.R-project.org/package=lmerTest). We used the functions lmer and glmer for the mixed-effects models of continuous and binary outcome variables, respectively. To obtain p-values for the fixed-effects test statistics in lmerTest, the calculation of the denominator degrees of freedom adopts Satterthwaite's approximation (cf. SAS proc mixed theory).

For analyses of individuals' trial-by-trial data coming from the BART, control

balloons were not included in the mixed-effects modeling. Control balloons merely constitute the baseline for the neural analyses and offer no insight into decision making in the BART.

Imaging data. For each person we extracted a mean signal for neural activations that were larger for risky compared with safe options from three regions of interest (ROI): the nucleus accumbens (NAcc), insula, and anterior cingulate cortex (ACC). Mean signal for a particular ROI was operationalized as the mean of all regression slopes extracted from all voxels contained in the structurally defined ROI. Concretely, for the BART, we extracted the mean of the regression slopes for the contrast *Pumps* > *Cash out*, and for monetary gambles *Accept* > *Reject*. All ROIs were structurally defined based on the Hammersmith atlas nr30r83 (http://brain-development.org/brain-atlases/adult-brain-maximum-probability-map-hammers-mith-atlas-n30r83-in-mni-space/).

Initial plotting of mean beta values extracted from the three ROIs indicated relatively normally distributed mean signals for both measures, except for a small number of possible outliers for signals extracted from ACC (n = 2) and insula (n = 1) in the BART, and ACC (n = 1) in monetary gambles. To account for any biasing effects, we computed robust regression analyses ("rlm" function in R package MASS (Venables and Ripley, 2002) using method "MM") and obtained a correlation coefficient of $r = 0.97$ ($p < 0.001$) between the coefficients from standard and robust analyses. Consequently, we only report estimates obtained from standard regression analyses. Results from ROI analyses were not confounded by laterality because similar findings were obtained from analyses extracting mean beta values from the two hemispheres separately. Concatenating the two runs from each paradigm to compute one neural index did not bias the results; comparable findings were observed for supplemental ROI analyses based on two separate runs per measure.

Corrections for multiple testing. To account for the number of analyses, we applied correction procedures to contrast analyses of neuroimaging data and individual differences

analyses of ROI data. All initial contrast analyses of neuroimaging data were conducted at the level of the whole brain. Accounting for multiple comparisons, a cluster-forming threshold ($p < .001$, uncorrected) was applied, followed by family-wise error correction at peak level ($p < .05$). To avoid putting too much emphasis on potentially uninformative single-activated voxels, we applied an extent threshold of a minimum of 100 contiguous voxels for all whole-brain group-level analyses. As we were agnostic regarding the potential overlap of voxels activated by both fMRI paradigms, we removed the extent threshold from our conjunction analysis.

To control for the number of analyses examining individual differences, we report which of the associations reach significance thresholds after family-wise error correction. For this purpose, we define four families of tests: (1) brain–brain associations (three tests); (2) brain–behavior associations for the BART (four tests; one whole-brain multiple regression analysis and three regression analyses based on extracted mean beta values from ROIs); (3) brain–behavior associations for monetary gambles (four tests; one whole-brain multiple regression analysis and three regression analyses based on extracted mean beta values from ROIs); and (4) brain–behavior associations across the two measures (four tests; one whole-brain multiple regression analysis plus three regression analyses based on extracted mean beta values from ROIs).

RESULTS

Neuroimaging results

In the BART, taking a risk (decisions to pump) versus going safe (decisions to cash out) was associated with increased activity in striatum (specifically bilateral NAcc), left anterior insula, and right precentral gyrus, extending into supplementary motor cortex (Table 4, Figure 2A); results for this contrast are comparable with previous results (Pletzer and Ortner, 2016). Due to the various cognitive and visual aspects surrounding cash-out

decisions, examination of the reverse main effect revealed widespread bilateral decreased activity, particularly in thalamus extending into hippocampal and parahippocampal regions and lateral occipital cortex. Because of the very short temporal delay between cash-out decisions and the subsequent visual feedback (~ 1 s), inclusion of the onset and duration of the visual feedback for cash-out decisions in the GLM did not achieve a more localized cash-out signal. Replication analyses of average activation differences for pumps on risky versus control balloons yielded results comparable with those of previous studies (Rao *et al.*, 2008; Schonberg *et al.*, 2012), including increased activation for peak coordinates located in bilateral ventral and dorsal striatum, bilateral anterior insular cortex, inter-hemispheric anterior cingulate and prefrontal cortex, as well as decreased activation in inter-hemispheric ventromedial prefrontal cortex, posterior cingulate and posterior parietal cortex, and bilateral parahippocampal gyrus and posterior insula (Table 4).

For monetary gambles, decisions to accept a risky gamble, when compared with decisions to reject, were associated with increased activation in several neural regions, including peak coordinates located in bilateral caudate extending into NAcc, right ACC, left angular gyrus, left inferior temporal and frontal gyrus (Table 4, Figure 2B). Examination of the reverse main effect yielded no significant deactivation. The pattern of activations found is comparable to those found in similar measures involving decisions from description (Barkley-Levenson et al., 2013; Tom et al., 2007; Wu et al., 2012).

Furthermore, replication analyses of average activation differences for pumps on reward versus control balloons in the BART (Table S1) yielded results comparable with previous studies (Rao *et al.*, 2008; Schonberg *et al.*, 2012; Yu *et al.*, 2016).

FIGURE LEGEND

Figure S1. Exemplary SPM design matrix for first (i.e., individual) level modeling of neural activation in the BART.

Figure S2. Exemplary SPM design matrix for first (i.e., individual) level modeling of neural activation in monetary gambles.

Figure S3. SPM design matrix for second (i.e., group) level modeling of main effects for the BART, monetary gambles, and their conjunction.

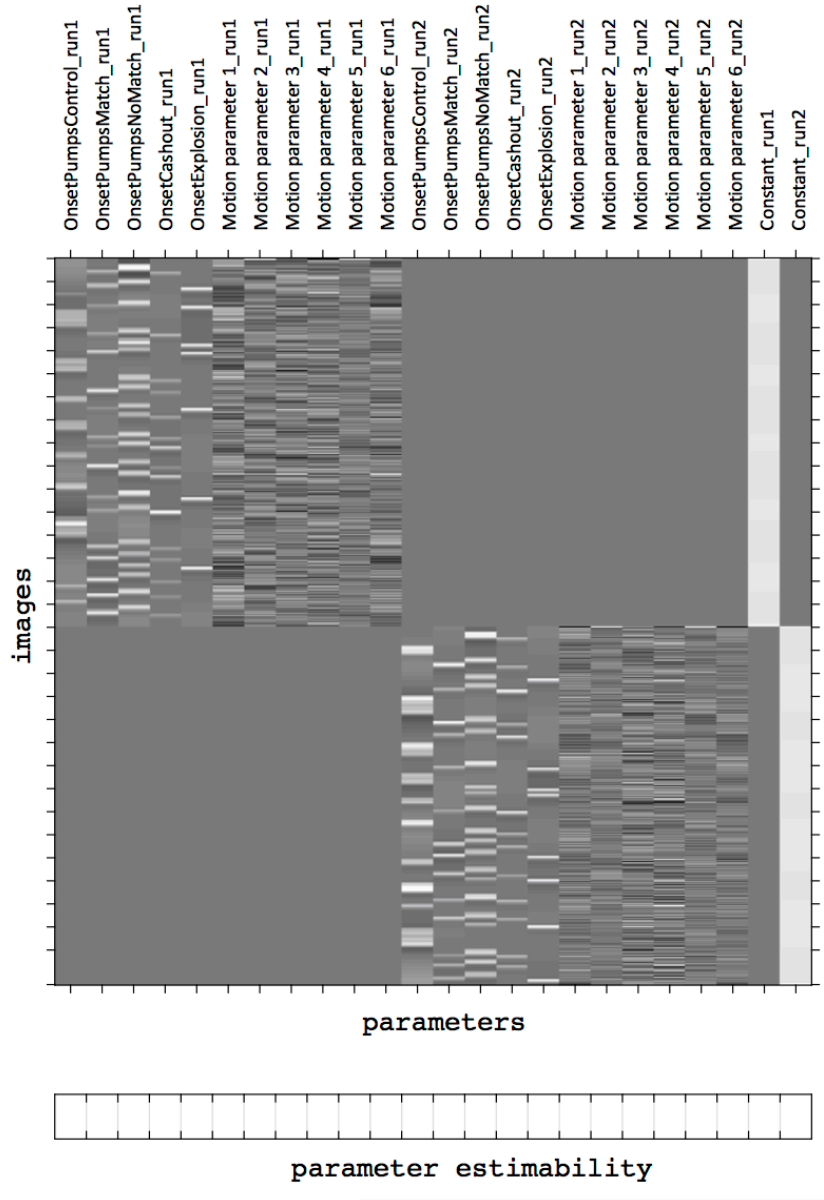

Figure S1. Exemplary SPM design matrix for first (i.e., individual) level modeling of neural activation in the BART.

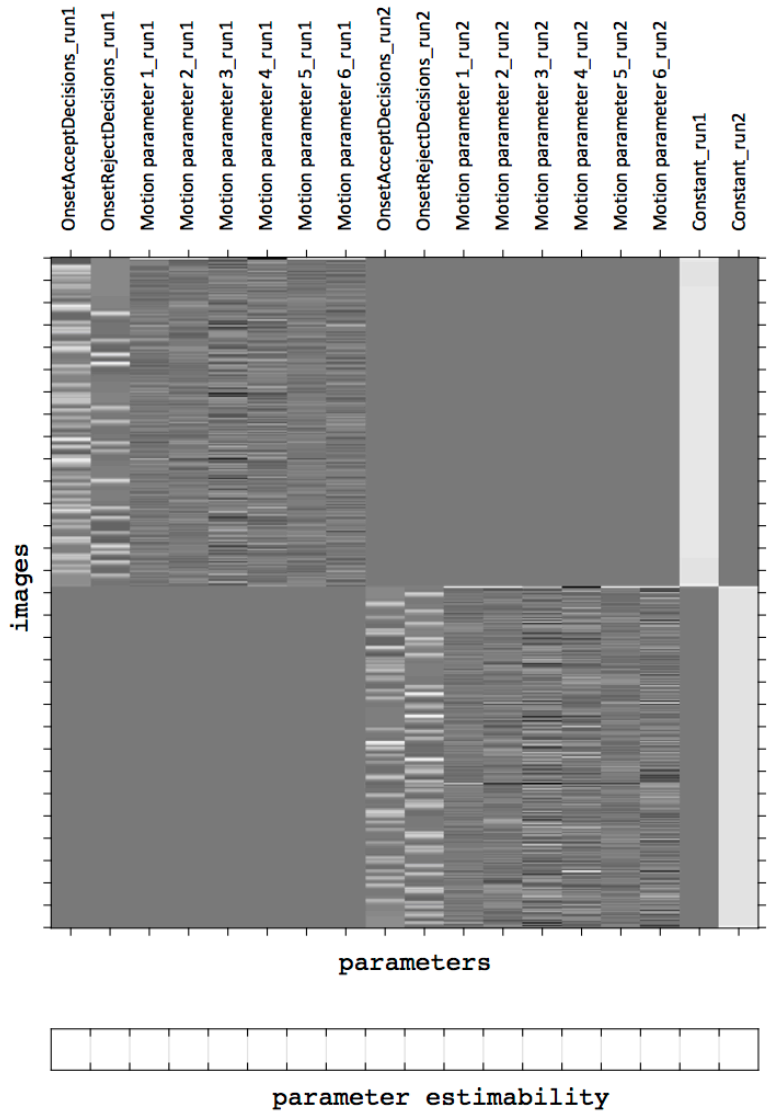

Figure S2. Exemplary SPM design matrix for first (i.e., individual) level modeling of neural activation in monetary gambles.

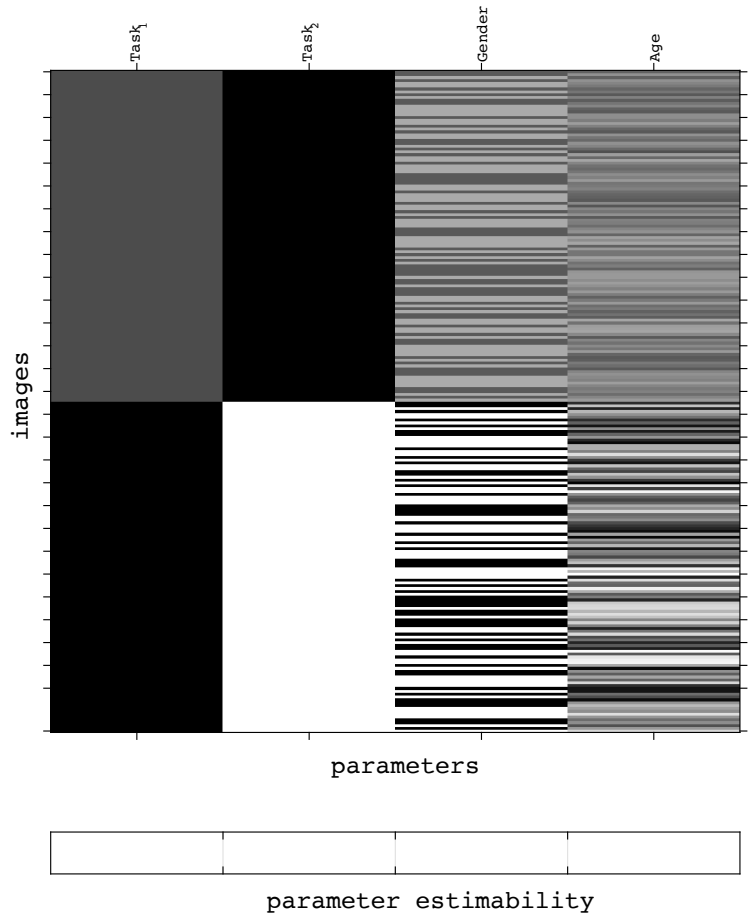

Figure S3. SPM design matrix for second (i.e., group) level modeling of main effects for the BART, monetary gambles, and their conjunction.

TABLE LEGEND

Table S1. Significant peak coordinates obtained from group-level contrast analyses for pumps on experimental (i.e., reward) balloons and control balloons in the BART.

Table S2. Significant peak coordinates obtained from multiple regression analysis to identify brain–behavior associations for monetary gambles.

Table S1. Significant peak coordinates obtained from group-level contrast analyses for pumps on experimental (i.e., reward) balloons and control balloons in the BART.

Region	R/L	MNI (mm) x	y	z	T	k
BART: $Pumps_{\_Risky} > Pumps_{\_Control}$						
Supplementary motor cortex	R	4	22	40	25.61	49140
Supramarginal gyrus	R	46	-42	44	17.26	5649
Occipital pole	L	-12	-102	-2	15.10	2845
BART: $Pumps_{\_Control} > Pumps_{\_Risky}$						
Angular gyrus	L	-48	-66	22	21.21	50828
Medial frontal cortex	L	-2	58	-12	18.65	5684

All analyses whole-brain, FWE cluster correction ($p<.05$), with $p<.001$ uncorrected voxel-wise (peak) threshold, controlled for effects of age and gender; k = number of voxels in cluster within which peak coordinate is located.

Table S2. Significant peak coordinates obtained from multiple regression analysis to identify brain–behavior associations for monetary gambles.

Region	R/L	MNI (mm) x	y	z	T	Voxels
Accept>Reject ~ Proportion accepted gambles: Positive association						
Occipital pole	R	24	-96	16	8.39	376
Central operculum	R	40	-12	20	8.06	406
Precentral gyrus	R	26	-22	52	7.85	1017
Occipital pole	L	-26	-96	14	7.23	262
Medial frontal cortex	R	10	48	-14	7.12	358
Middle temporal gyrus	L	-56	-10	-20	6.75	437
Superior temporal gyrus	R	62	-30	12	6.57	205
Parietal operculum	L	-38	-40	18	6.14	101
Superior temporal gyrus	R	60	-8	-6	6.06	153
Accept>Reject ~ Proportion accepted gambles: Negative association						
Anterior insula	R	36	24	-4	12.89	10048
Anterior insula	L	-34	18	-6	11.82	1155
Supramarginal gyrus	R	42	-40	42	11.61	4519
Supramarginal gyrus	L	-50	-38	46	10.60	2888
Middle cingulate gyrus	L	-2	-26	30	8.22	313
Precentral gyrus	L	-52	8	28	7.76	700
Inferior temporal gyrus	R	56	-56	-14	7.36	240
Precentral gyrus	L	-28	-12	52	7.29	321

All analyses whole-brain, FWE cluster correction ($p<.05$), with $p<.001$ uncorrected voxel-wise (peak) threshold, and cluster extent threshold $k>100$, controlled for effects of age and gender; k = number of voxels in cluster within which peak coordinate is located.

REFERENCES

Ashburner, J., Friston, K.J. (2005). Unified segmentation. *NeuroImage*, **26**, 839–51

Barkley-Levenson, E.E., Van Leijenhorst, L., Galván, A. (2013). Behavioral and neural correlates of loss aversion and risk avoidance in adolescents and adults. *Developmental Cognitive Neuroscience*, **3**, 72–83

Canessa, N., Crespi, C., Motterlini, M., et al. (2013). The functional and structural neural basis of individual differences in loss aversion. *The Journal of Neuroscience*, **33**, 14307–17

Frey, R., Pedroni, A., Mata, R., et al. (2017). Risk preference shares the psychometric structure of major psychological traits. *Science Advances*, **3**, 1–13

Frey, R., Rieskamp, J., Hertwig, R. (2015). Sell in may and go away? Learning and risk taking in nonmonotonic decision problems. *Journal of Experimental Psychology: Learning Memory and Cognition*, **41**, 193–208

Lejuez, C.W., Read, J.P., Kahler, C.W., et al. (2002). Evaluation of a behavioral measure of risk taking: the Balloon Analogue Risk Task (BART). *Journal of Experimental Psychology. Applied*, **8**, 75–84

Mamerow, L., Frey, R., Mata, R. (2016). Risk Taking Across the Life Span: A Comparison of Self-Report and Behavioral Measures of Risk Taking. *Psychology and Aging*, **31**

Meermann, R., Vandereycken, W. (1987). *Therapie der Magersucht und Bulimia nervosa*. Berlin: de Gruyter.

Paulhus, D.L., Vazire, S. (2007). The Self-Report Method. In: R. W. Robins, R. C. Fraley, R. F. Krueger (eds). *Handbook of Research Methods in Personality Psychology*. New York: Guilford, p. 224–39.

Pleskac, T.J. (2008). Decision Making and Learning While Taking Sequential Risks. *Journal of Experimental Psychology: Learning Memory and Cognition*, **34**, 167–85

Pletzer, B., Ortner, T.M. (2016). Neuroimaging supports behavioral personality assessment:

Overlapping activations during reflective and impulsive risk taking. *Biological Psychology*, **119**, 46–53

Pudel, V., Westenhöfer, J. (1989). *Fragebogen zum Essverhalten (FEV): Handanweisung*. Göttingen, Toronto, Zürich: Verlag für Psychologie, Hogrefe.

Rao, H., Korczykowski, M., Pluta, J., et al. (2008). Neural correlates of voluntary and involuntary risk taking in the human brain: An fMRI Study of the Balloon Analog Risk Task (BART). *NeuroImage*, **42**, 902–10

van Ravenzwaaij, D., Dutilh, G., Wagenmakers, E.J. (2011). Cognitive model decomposition of the BART: Assessment and application. *Journal of Mathematical Psychology*, **55**, 94–105

Rolison, J.J., Hanoch, Y., Wood, S. (2012). Risky decision making in younger and older adults: the role of learning. *Psychology and Aging*, **27**, 129–40

Schmidt, R.E., Gay, P., D'Acremont, M., et al. (2008). A German adaptation of the upps impulsive behavior scale: Psychometric properties and factor structure. *Swiss Journal of Psychology*, **67**, 107–12

Schonberg, T., Fox, C.R., Mumford, J.A., et al. (2012). Decreasing ventromedial prefrontal cortex activity during sequential risk-taking: An FMRI investigation of the balloon analog risk task. *Frontiers in Neuroscience*, **6**, 1–11

Sokol-Hessner, P., Camerer, C.F., Phelps, E.A. (2013). Emotion regulation reduces loss aversion and decreases amygdala responses to losses. *Social Cognitive and Affective Neuroscience*, **8**, 341–50

Tom, S.M., Fox, C.R., Trepel, C., et al. (2007). The neural basis of loss aversion in decision-making under risk. *Science*, **315**, 515–18

Venables, W.N., Ripley, B.D. (2002). *Modern Applied Statistics with S*. Fourth edi. New York: Springer.

Wallsten, T.S., Pleskac, T.J., Lejuez, C.W. (2005). Modeling Behavior in a Clinically Diagnostic Sequential Risk-Taking Task. *Psychological Review*, **112**, 862–80

Westenhöfer, J. (1992). *Gezügeltes Essen und Störbarkeit des Essverhaltens.* Göttingen: Verlag für Psychologie, Hogrefe.

Wu, C.C., Sacchet, M.D., Knutson, B. (2012). Toward an affective neuroscience account of financial risk taking. *Frontiers in Neuroscience*, **6**, 1–10

Yarkoni, T. (2009). Big correlations in little studies. Inflated fMRI correlations reflect low statistical power - commentary on Vul et al. (2009). *Perspectives on Psychological Science*, **4**, 294–98

Yu, J., Mamerow, L., Lei, X., et al. (2016). Altered Value Coding in the Ventromedial Prefrontal Cortex in Healthy Older Adults. *Frontiers in Aging Neuroscience*, **8**